

Multi-Objective Optimal Design of Surface-Mounted Permanent Magnet Motor Using NSGA-II

S. Mendaci¹, H. Allag², and M. R. Mekideche²

¹Laboratory of Automatics and Informatics of Guelma-LAIG
University of Guelma, Guelma, 24000, Algeria
mendaci.sofiane@yahoo.fr

²Department of Electrical Engineering
University of Jijel, 18000, Algeria
allag_hic@yahoo.fr, mek_moh@yahoo.fr

Abstract — This paper presents a highly structured procedure for multi-objective optimal design of radial surface Permanent-Magnet Synchronous Motor (PMSM). Firstly, a detailed analytical model based on the resolution of Maxwell's equations using the separation of variables method is presented. From the same model, analytical expressions of four constraint functions dedicated for the optimal design of the PMSM are developed. These constraints are: electromagnetic torque, back electromotive force (back-EMF), flux density saturation in stator/rotor yoke and saturation in stator tooth. Then, the Non-dominated Sorting Genetic Algorithm-II (NSGA-II) is employed to optimize the multi-objective problem formed by two objective functions (weight and power loss of the motor) and different constraints. Finally, the finite element method is used to validate the designed 30 kW PMSM.

Index Terms — Analytical model, finite elements, NSGA-II, optimal design, permanent magnet synchronous motor.

I. INTRODUCTION

In recent years, the manufacturers of electrical machines have shown a growing interest for permanent magnet synchronous machines (PMSMs). This interest is mainly due to the high efficiency, high reliability, high power density, small size and decreasing cost of magnets. Different topologies of PM machines are available; e.g., radial flux machines, axial flux machines and transversal flux machines [1]. However, the performances of PMSMs are greatly depends on their optimal design and control.

The design and dimensioning of an electromechanical actuator calls into play a great number of parameters which are subject to the laws which describe physical phenomena on the one hand and to the

specifications of the schedule of conditions on the other hand. In the practice, many electromagnetic optimization problems are solved by means of highly accurate models (e.g., finite element model) with different optimization algorithms. However, these approaches are computationally expensive, especially when stochastic optimization algorithms are used [2]. As an alternative, very simplified analytical models are useful tools for first evaluation and design optimization. They are proved fast, but not very accurate [3].

In this paper, the authors attempt to provide helpful tools for the fast analysis and multi-objective optimal design of PMSMs. Prior to the optimization, an analytical model, sufficiently accurate and fast, based on the resolution of Maxwell's equations using the separation of variables method is presented. Then, the design processes was formulated as a multi-objective optimization problem and solved by NSGA-II method. Finally, validity of the proposed methodology is confirmed through the finite element analysis of the designed 30 kW PMSM.

II. DEVELOPMENT OF THE ANALYTICAL MODEL

The general configuration of a slotted surface-mounted permanent magnet motor considered in the present work is shown in Fig. 1.

The analytical method used in this paper is based on analysis of 2-D model in polar coordinates. The following assumptions are made [4-7]:

- The stator and rotor cores are assumed to be infinitely permeable.
- End effect and saturation are neglected.
- Permanent magnets have a linear demagnetization characteristic.
- Eddy current effects are neglected (no eddy current loss in the magnets or armature windings).

- Stator current source is represented by a current sheet distributed over the stator inner radius.

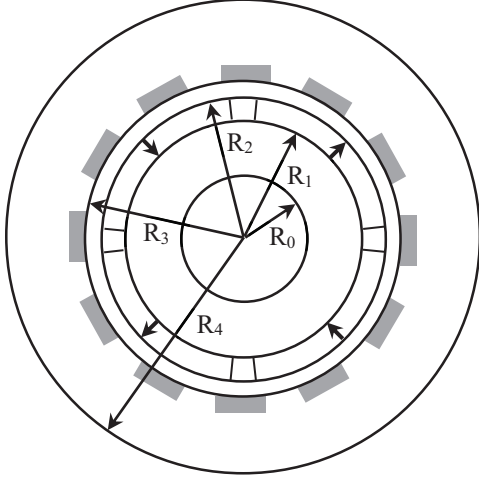


Fig. 1. Cross sectional view of the studied PMSM.

In the above considerations, the calculation region can be classified into two parts: PMs (Region I), and air-gap (Region II). The flux density and field intensity are expressed as:

$$\text{In Region I:} \quad \vec{B} = \mu_0 \vec{H}. \quad (1)$$

$$\text{In Region II:} \quad \vec{B} = \mu_0 \mu_r \vec{H} + \mu_0 \vec{M}, \quad (2)$$

where μ_r is the relative recoil permeability, \vec{M} is the magnetization vector of permanent magnets. The direction of \vec{M} depends on the orientation and magnetization of permanent magnets. In polar coordinates, the magnetization vector \vec{M} is expressed as:

$$\vec{M} = M_r \vec{e}_r + M_\theta \vec{e}_\theta. \quad (3)$$

The governing field equations are, in terms of the Coulomb gauge, $\nabla \cdot \vec{A} = 0$, as follows:

$$\text{In Region I:} \quad \nabla^2 \vec{A} = -\mu_0 \nabla \times \vec{M}. \quad (4)$$

$$\text{In Region II:} \quad \nabla^2 \vec{A} = 0. \quad (5)$$

\vec{A} (the magnetic vector potential) only has A_z component which is independent of z (infinitely long machine in axial direction).

By using the method of separating variables, the general solution of (4) and (5) can be expressed as:

$$A_z^I = \sum_{g=-\infty}^{+\infty} (C_1 r^{gp} + C_2 r^{-gp} + A_p) e^{jgp\theta}, \quad (6)$$

$$A_z^{II} = \sum_{g=-\infty}^{+\infty} (C_3 r^{gp} + C_4 r^{-gp}) e^{jgp\theta}, \quad (7)$$

where A_p is the particular solution of (4) for the permanent magnets region, given by:

$$A_p(r) = \begin{cases} \mu_0 \frac{jgpM_{r,g} - M_{\theta,g}}{1-(gp)^2} r & \text{if } gp \neq 1 \\ \mu_0 \frac{jgpM_{r,g} - M_{\theta,g}}{2} r \ln(r) & \text{if } gp = 1 \end{cases}, \quad (8)$$

where $M_{r,g}$ and $M_{\theta,g}$ are the complex Fourier coefficients of the two components $M_r(\theta)$ and $M_\theta(\theta)$ of the magnetization vector \vec{M} .

$$M_r(\theta) = \sum_{g=-\infty}^{+\infty} M_{r,g} e^{jgp(\theta-\Omega t)}. \quad (9)$$

$$M_\theta(\theta) = \sum_{g=-\infty}^{+\infty} M_{\theta,g} e^{jgp(\theta-\Omega t)}, \quad (10)$$

where p is the pole pair number and Ω is the rotor speed.

In (6) and (7), C_1 , C_2 , C_3 , and C_4 are constants to be determined by applying the boundary conditions on the interface between rotor and PMs (i.e., $r=R_1$), PMs and air gap (i.e., $r=R_2$) and between the air-gap and stator (i.e., $r=R_3$). These conditions can be defined as:

$$\begin{cases} H_\theta^I(R_1, \theta) = 0. \\ H_\theta^I(R_2, \theta) = H_\theta^{II}(R_2, \theta). \\ B_r^I(R_2, \theta) = B_r^{II}(R_2, \theta). \\ H_\theta^{II}(R_3, \theta) = -\mu_0 J. \end{cases} \quad (11)$$

J is the total current density vector given by:

$$J(\theta, t) = \sum_{n=1}^m J_n = \sum_{n=1}^m I_n C_n, \quad (12)$$

where m is the number of phase windings and J_n is the current density for phase n given by the product of the conductor density $C_n(\theta)$ and the stator current I_n , with:

$$C_n(\theta) = \sum_{g=-\infty}^{+\infty} \frac{S_g}{2j} e^{jgp(\theta - \frac{(n-1)2\pi}{p m})}. \quad (13)$$

The Fourier coefficient S_g is determined by taking into account the windings characteristics. In the case of diametric winding, S_g is given by:

$$S_g = 2\gamma \sum_{k=1}^{\frac{N_{spp}}{2}} \cos\left((2k-1)gp \frac{P_t}{2}\right). \quad N_{spp} \text{ is even} \quad (14)$$

$$S_g = \gamma \left(1 + 2 \sum_{k=1}^{\frac{N_{spp}-1}{2}} \cos(kgpP_t) \right), \quad N_{spp} \text{ is odd} \quad (15)$$

where N_{spp} is the number of slots per pole and per phase, P_t is the stator tooth-pitch and γ given by:

$$\gamma = \frac{4N_c}{R_3 b_s} \sin\left(g \frac{\pi}{2}\right) \sin\left(gp \frac{b_s}{2}\right), \quad (16)$$

where N_c is the number of conductors in one slot and b_s is the slot width.

In the general case, the total stator current density can be written as a Fourier series:

$$J(\theta, t) = \sum_{g=-\infty}^{+\infty} J_g(t) e^{jgp\theta}, \quad (17)$$

where J_g is the complex Fourier coefficient given by:

$$J_g(t) = \frac{S_g}{2j} \sum_{n=1}^m I_n(t) e^{-jg(n-1)\frac{2\pi}{m}}. \quad (18)$$

The resolution of the above system (11) gives the constants $C_1, C_2, C_3,$ and C_4 . They can be expressed as:

$$C_1 = \mu_0 \left(P_2 M_{r,g} + P_3 M_{\theta,g} \right) e^{-j(gp\Omega t - \frac{\pi}{2})} + P_1 S_g \sum_{n=1}^m I_n(t) e^{-j(g(n-1)\frac{2\pi}{m} + \frac{\pi}{2})}. \quad (19)$$

$$C_2 = \mu_0 \left(D_2 M_{r,g} + D_3 M_{\theta,g} \right) e^{-j(gp\Omega t - \frac{\pi}{2})} + D_1 S_g \sum_{n=1}^m I_n(t) e^{-j(g(n-1)\frac{2\pi}{m} + \frac{\pi}{2})}. \quad (20)$$

$$C_3 = \mu_0 \left(E_2 M_{r,g} + E_3 M_{\theta,g} \right) e^{-j(gp\Omega t - \frac{\pi}{2})} + E_1 S_g \sum_{n=1}^m I_n(t) e^{-j(g(n-1)\frac{2\pi}{m} + \frac{\pi}{2})}. \quad (21)$$

$$C_4 = \mu_0 \left(F_2 M_{r,g} + F_3 M_{\theta,g} \right) e^{-j(gp\Omega t - \frac{\pi}{2})} + E_1 S_g \sum_{n=1}^m I_n(t) e^{-j(g(n-1)\frac{2\pi}{m} + \frac{\pi}{2})}, \quad (22)$$

where

$$P_1 = \mu_0 R_3^{1-gp} L_1. \quad (23)$$

$$P_2 = gp \frac{L_1}{2} \left[\frac{df(R_1)}{dr} L_2 + \frac{df(R_2)}{dr} L_3 + f(R_2) L_4 \right]. \quad (24)$$

$$P_3 = \frac{L_1}{2} \left[\left(\frac{df(R_1)}{dr} - 1 \right) L_2 + \left(\frac{df(R_2)}{dr} - 1 \right) L_3 + f(R_2) L_4 \right]. \quad (25)$$

$$D_1 = P_1 R_1^{2gp}. \quad (26)$$

$$D_2 = P_2 R_1^{2gp} + \frac{df(R_1)}{dr} \frac{R_1^{1+gp}}{2}. \quad (27)$$

$$D_3 = P_3 R_1^{2gp} + \left(\frac{df(R_1)}{dr} - 1 \right) \frac{R_1^{1+gp}}{2gp}. \quad (28)$$

$$E_1 = P_1. \quad (29)$$

$$E_2 = P_2 + \frac{gpR_2^{-gp}}{4} f(R_2) + \frac{df(R_2)}{dr} \frac{R_2^{1-gp}}{4}. \quad (30)$$

$$E_3 = P_3 + \frac{R_2^{-gp}}{4} f(R_2) + \left(\frac{df(R_2)}{dr} - 1 \right) \frac{R_2^{1-gp}}{4gp}. \quad (31)$$

$$F_1 = D_1. \quad (32)$$

$$F_2 = D_2 + \frac{gpR_2^{gp}}{4} f(R_2) - \frac{df(R_2)}{dr} \frac{R_2^{1+gp}}{4}. \quad (33)$$

$$F_3 = D_3 + \frac{R_2^{gp}}{4} f(R_2) - \left(\frac{df(R_2)}{dr} - 1 \right) \frac{R_2^{1+gp}}{4gp}, \quad (34)$$

with

$$L_1 = \frac{1}{2gp \left(1 - R_1^{2gp} R_3^{-2gp} \right)}. \quad (35)$$

$$L_2 = 2R_1^{1+gp} R_3^{-2gp}. \quad (36)$$

$$L_3 = - \left(R_2^{1-gp} + R_2^{1+gp} R_3^{-2gp} \right). \quad (37)$$

$$L_4 = gp \left(R_2^{gp} R_3^{-2gp} - R_2^{-gp} \right). \quad (38)$$

$$f(r) = \begin{cases} \frac{r}{1-(gp)^2} & \text{if } gp \neq 1 \\ \frac{r}{2} \ln(r) & \text{if } gp = 1 \end{cases}. \quad (39)$$

Hence, the magnetic vector potential is completely defined in the two regions by (6) and (7). Therefore, the flux density in the air-gap and PMs is given by:

$$B_r^i(r, \theta, t) = 2 \sum_{g=1}^{\infty} \left[\mu_0 \left(N_{2,r}^i M_{r,g} + N_{3,r}^i M_{\theta,g} \right) \cos(gp(\Omega t - \theta)) - N_{1,r}^i S_g \sum_{n=1}^m I_n(t) \cos \left(g \left(p\theta - (n-1) \frac{2\pi}{m} \right) \right) \right] \quad (40)$$

$$B_\theta^i(r, \theta, t) = 2 \sum_{g=1}^{\infty} \left[\mu_0 \left(T_{2,r}^i M_{r,g} + T_{3,r}^i M_{\theta,g} \right) \sin(gp(\Omega t - \theta)) + T_{1,r}^i S_g \sum_{n=1}^m I_n(t) \sin \left(g \left(p\theta - (n-1) \frac{2\pi}{m} \right) \right) \right], \quad (41)$$

where $i=I,II$ design the concerned region.

$$N_{l,r}^i = \frac{-gp}{r} P_{l,r}^i. \quad (42)$$

$$T_{l,r}^i = -\frac{dP_{l,r}^i}{dr}, \quad \text{with } l=1,2,3 \quad (43)$$

and

$$P_{1,r}^1 = P_1 r^{gp} + D_1 r^{-gp}. \quad (44)$$

$$P_{2,r}^1 = P_2 r^{gp} + D_2 r^{-gp} + \frac{gp}{2} f(r). \quad (45)$$

$$P_{3,r}^1 = P_3 r^{gp} + D_3 r^{-gp} + \frac{1}{2} f(r), \quad (46)$$

$$P_{1,r}^2 = E_1 r^{gp} + F_1 r^{-gp}. \quad (47)$$

$$P_{2,r}^2 = E_2 r^{gp} + F_2 r^{-gp}. \quad (48)$$

$$P_{3,r}^2 = E_3 r^{gp} + F_3 r^{-gp}. \quad (49)$$

To improve the precision of this analytical model, Carter's coefficient K_c is applied to compensate the slots

effects. In this case, a new air gap length e_c is defined by [8]:

$$e_c = K_c e, \quad (50)$$

where

$$K_c \approx \frac{P_t}{\left(P_t - \frac{b_s^2}{5e + b_s} \right)}, \quad \text{and} \quad P_t = \frac{2\pi R_s}{2pmN_{spp}}. \quad (51)$$

III. CONSTRAINTS DEDUCED FROM THE PROPOSED MODEL

A. Torque constraint

The torque developed on the motor can be obtained by calculating the Maxwell stress tensors in the air-gap [4,6,7]:

$$T_m = \frac{LR_2^2}{\mu_o} \int_0^{2\pi} B_r^{\parallel} B_{\theta}^{\parallel} d\theta, \quad (52)$$

where L is the axial length.

Incorporating (40) and (41) in (52) and integrating on the tangential direction yields to the final expression of the torque in terms of field sources ($M_{r,g}$, $M_{\theta,g}$ and I_n):

$$T_m = \frac{8\pi L p^2}{\mu_o} \left[\sum_{g=1}^{\infty} g^2 N_g S_g \times \left(\sum_{n=1}^m I_n(t) \sin \left(gp \left(\Omega t - \frac{(n-1)2\pi}{p} \right) \right) \right) \right], \quad (53)$$

where

$$N_g = \mu_o (E_1 F_2 - E_2 F_1) M_{r,g} + \mu_o (E_1 F_3 - E_3 F_1) M_{\theta,g}. \quad (54)$$

The torque expression (53) depends on the design parameters. Therefore, this expression can be used as objective function or as constraint in the preliminary PM motor design.

B. Back electromotive force constraint

The back-EMF created by the permanent magnet can be obtained by Faraday's law:

$$E_n(t) = -\frac{\partial \Phi_{n0}(t)}{\partial t}, \quad (55)$$

where $\Phi_{n0}(t)$ is the phase n flux linkage created by PMs.

Based on Stokes theorem, the flux linkage $\Phi_{n0}(t)$ is calculated by:

$$\Phi_{n0}(t) = \int_s B ds = \int_{\Gamma} A dl = LR_3 \int_0^{2\pi} A_z^{\parallel}(R_3, \theta, t) C_n(\theta) d\theta. \quad (56)$$

After the substitution and the simplification, the final expression of $\Phi_{n0}(t)$ is given by:

$$\Phi_{n0}(t) = 2\pi R_3 L \sum_{g=1}^{\infty} \Phi_{AP}(R_3) \cos \left(g \left(p\Omega t - (n-1) \frac{2\pi}{m} \right) \right), \quad (57)$$

with

$$\Phi_{AP}(R_3) = -\mu_o S_g \left[P_{2,r}^2(R_3) M_{r,g} + P_{3,r}^2(R_3) M_{\theta,g} \right]. \quad (58)$$

From the equations (55) and (57), the back-EMF created by PMs is given by:

$$E_n(t) = 2\pi R_3 L p \Omega \times \sum_{g=1}^{\infty} g \Phi_{AP}(R_3) \sin \left(g \left(p\Omega t - (n-1) \frac{2\pi}{m} \right) \right). \quad (59)$$

C. Stator and rotor yoke saturation constraint

The definition of the no saturation constraint of rotor/stator yoke needs the acknowledgement of the flux density in these regions.

The Fig. 2 shows that the magnetic flux in rotor yoke $\Phi_r(t)$ is equal to the flux in a half PM pole $\Phi_{hp}(t)$:

$$\Phi_r(t) = \Phi_{hp}(t). \quad (60)$$

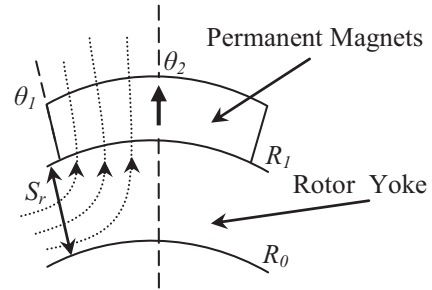


Fig. 2. Flux density trajectory in rotor yoke.

From the Fig. 2, the rotor flux yoke is given by:

$$\Phi_r(t) = B_r(t) S_r = L (R_1 - R_0) B_r(t), \quad (61)$$

where $B_r(t)$ is the tangential component of flux density in the rotor and S_r is the cross section area of the rotor yoke.

In other hand, the magnetic flux in half PM pole at R_1 is given by:

$$\Phi_{hp}(t) = \int A_z^I(R_1) dl = L \left[A_z^I(R_1, \theta_2, t) - A_z^I(R_1, \theta_1, t) \right]. \quad (62)$$

By using (60), (61) and (62) we obtain the analytical expression of the flux density in the rotor/stator yoke (supposed to have the same dimensions):

$$B_r(t) = \frac{\left[A_z^I(R_1, \theta_2, t) - A_z^I(R_1, \theta_1, t) \right]}{(R_1 - R_0)}. \quad (63)$$

Usually, to avoid excessive saturation, the maximum flux density of iron core is limited to the range 1.6-1.9 T [3].

D. Stator tooth saturation constraint

In the case of slotted motor, we can introduce a constraint for no stator tooth saturation.

If we neglecting the flux leakage, the flux in the stator tooth $\Phi_{tooth}(t)$ is given by:

$$\Phi_{tooth}(t) = \frac{2\Phi_{hp}(t)}{mN_{spp}}. \quad (64)$$

The stator tooth flux can be also expressed as:

$$\Phi_{tooth}(t) = B_{st}(t)S_{st}, \quad (65)$$

where $B_{st}(t)$ and S_{st} are the flux density and the small cross section area of stator tooth respectively.

By using (62), (64) and (65) we obtain the expression of the flux density in the stator tooth as:

$$B_{st}(t) = \frac{2L \left[A_z^I(R_I, \theta_2, t) - A_z^I(R_I, \theta_1, t) \right]}{S_{st} m N_{spp}}. \quad (66)$$

IV. DESIGN OPTIMIZATION PROCEDURE

A. Optimization problem definition

In order to present the design optimization procedure of surface mounted PMSM, based on the above analytical model, we designed a 30 kw PMSM with the following assumptions: 10 poles, 30 slots, one slot per pole and per phase ($N_{spp}=1$), based speed $w_{base}=1500$ rpm, maximal speed $w_{max}=4500$ rpm, current density $J=7$ A/mm², NdFeB magnets with a remanent flux density of 1.2 and a relative permeability of 1.

The objective functions fixed for this optimization are:

- *Minimizing the weight of the motor (M).*
- *Maximizing the efficiency by minimizing the power loss (PL).*

The mass M of the active part is given by:

$$M = M_C + M_{PM} + M_S + M_R, \quad (67)$$

where M_C , M_{PM} , M_S and M_R are respectively the weight of: the copper, the permanent magnet, the stator iron and the rotor iron. These masses are given by the following expressions:

$$M_C = 2 pm N_{spp} S_s \left(L + 1.6 \left(\frac{2 \pi R_3}{2 p} \right) \right) \rho_{copper}. \quad (68)$$

$$M_{PM} = \pi (R_2^2 - R_1^2) L K_{PM} \rho_{PM}. \quad (69)$$

$$M_S = \left(\pi (R_4^2 - R_3^2) - 2 pm N_{spp} P_s b_s \right) L \rho_{iron}. \quad (70)$$

$$M_R = \pi (R_i^2 - R_o^2) L \rho_{iron}, \quad (71)$$

where S_s is the section of copper in slot, K_{PM} is the magnet-arc to pole-pitch ratio and P_s is the slot depth. Also, ρ_{copper} , ρ_{PM} and ρ_{iron} are respectively the density of: copper, permanent magnet and iron.

The power loss in the PMSM is given by the sum of the loss in the stator winding (P_{Lcop}) and the core loss (hysteresis P_{Lhys} and eddy current loss P_{Leddy}) [3]:

$$P_L(W) = P_{Lcop} + (P_{Lhys} + P_{Leddy}) \mathcal{V}_{volume_iron}, \quad (72)$$

with

$$P_{Lcop}(W) = 3 R_s I_{neff}^2. \quad (73)$$

$$P_{Lhys}(W \cdot m^{-3}) = K_{hys} B^\beta W_s. \quad (74)$$

$$P_{Leddy}(W \cdot m^{-3}) = \frac{2}{T} \int_0^T K_{eddy} \left(\frac{dB}{dt} \right)^2 dt, \quad (75)$$

where K_{hys} and K_{eddy} are the classical eddy and hysteresis loss coefficients which can be calculated at various frequencies and flux densities from curve fitting of manufacturer data sheets.

Finally, the multi-objective constrained optimization problem is defined as:

$$\text{Minimize:} \quad \text{weight and power loss} \quad (76)$$

Subject to the following constraints:

- *Electromagnetic torque, $T = 191$ Nm*
- *Back-EMF at maximum speed, $E_{max} \leq 500$ V*
- *Tator/rotor yoke flux density, $B_{yoke} \leq 1.6$ T*
- *Tator tooth flux density, $B_{tooth} \leq 1.6$ T*

Firstly, before solving the above problem (76), we have dimensioning our PMSM by using the direct method proposed in [3]. From the obtained initial dimensioning, we have chosen seven variables, given in Table 1 with their exploration domain, to solve the final problem (76).

Table 1: The exploration domain for each variable

Variable	Symbol	Min	Max
Inner radius of the rotor yoke (m)	R_o	0.07	0.13
Axial length (m)	L	0.06	0.12
Thickness of magnet (m)	L_{PM}	0.003	0.006
Radius of the rotor yoke surface (m)	R_I	0.13	0.2
Magnet-arc to pole-pitch ratio	K_{PM}	0.6	0.9
Slot-opening to slot-pitch ratio	K_{So}	0.3	0.6
Slot depth (m)	P_s	0.02	0.03

B. Non-dominated sorting genetic algorithm

To optimize the constrained multi-objective problem (76), the Non-dominated Sorting Genetic Algorithm II (NSGA-II) is applied.

The NSGA-II is one of the most widely used algorithms in various engineering optimization processes due to its simplicity, parameter less-niching, better convergence near the true Pareto-optimal front, better spread of solutions and low computational requirements [9-11].

The main NSGA-II procedure is given below:

- Create a random population P_0 (of size N).
- Sort P_0 according to non-domination. Each solution is assigned a new fitness equal to its non-domination rank (1 is the best level). Then, use selection, recombination, and mutation to create the offspring population Q_0 (of size N) from P_0 .
- While generation count is not reached, combine parent and offspring population to form the combined population R_t (of size $2N$).

- Perform non-dominated sort on the population R_t . Then, calculate the crowding-distance for each solution. It is calculated by the size of the largest cuboid enclosing each solution without including any other point [9,10].
- Construct the next parent population P_{t+1} by choosing only the best N solutions from R_t . Each solution is evaluated by using its front rank as primary criteria and crowding-distance as secondary if it belongs to the last selected front.
- Use the new parent population P_{t+1} (of size N) for selection, crossover, and mutation to create a new population Q_{t+1} (of size N). We note that the selection criterion between two solutions is now based on the crowded-comparison operator (If the two solutions are from different fronts, we select the solution with lowest front rank. But, if they are from the same front, we select the individual with the highest crowding distance).

In this paper, the following parameters are used: population size $N=200$, maximum number of generations is 4000, mutation probability is 0.1, and crossover probability is 0.9. The variables are treated as real numbers and the Breeder Genetic Crossover (BGX) and the real-parameter mutation operator are used [12].

C. Results

The multi-objective optimization takes 70 minutes with NSGA-II method. The Pareto-optimal front for motor weight versus total loss is obtained as shown in Fig. 3.

The variables and the performances of the initial (MI) and two optimized PMSMs (MW: minimum weight and MP: minimum power loss) are presented in Table 2. As shown, the optimized motors characteristics are significantly better than the initial motor. The mass and the total power loss are minimized and are smaller than that of the initial motor. Also, the four optimization constraints are respected, especially the value of the electromagnetic torque.

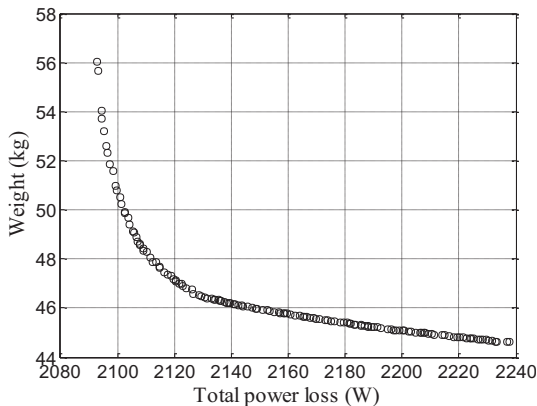


Fig. 3. Pareto-optimal front.

Table 2: Comparison between the initial and optimized PMSMs

Variables and Performances	MI	MW	MP
R_o (m)	0.0955	0.1147	0.113
L (m)	0.0955	0.06	0.0695
L_{PM} (m)	0.0077	0.006	0.006
R_l (m)	0.1251	0.1428	0.1439
K_{PM}	0.833	0.6	0.6
K_{So}	0.5	0.4027	0.3042
P_s	0.0239	0.0272	0.03
Number of conductors in slot	8	12	10
Current (A)	100	105	105
Electromagnetic torque (Nm)	177.7	191	191
Back-EMF at maximum speed (V)	448.9	464.3	461.5
Maximum yoke flux density (T)	1.9	1.6	1.5
Maximum tooth flux density (T)	1.4	1.6	1.4
Mass (kg)	61.3	44.6	56
Total power loss (W)	3955	2237.7	2092.5
Efficiency	0.8835	0.9306	0.9348

In order to validate the proposed design procedure, the performances of MW designed machine have been compared with 2D finite element simulations (2D FE). Figures 4 and 5 show respectively the electromagnetic torque and the back-EMF. We can observe that the mean torque and the maximum value of the back-EMF obtained by FE simulations are in good agreement with analytical results. However, the small error between the two models and the ripples in the torque and in the back-EMF are due to the effect of stator slots, considered in implicit way in the analytical model by Carter's coefficient.

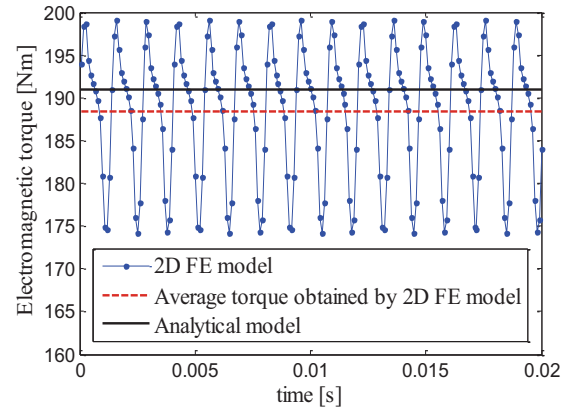


Fig. 4. Electromagnetic torque obtained for $\omega=1500$ rpm (the base speed).

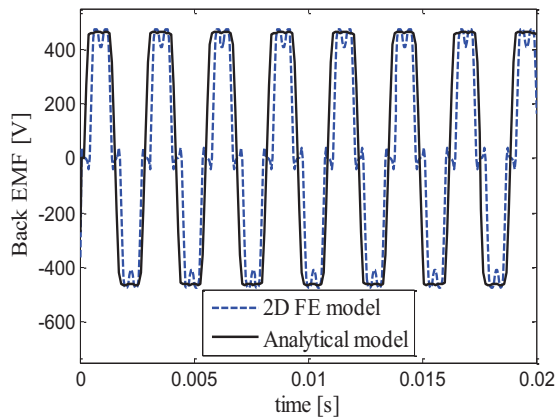


Fig. 5. Back-EMF obtained for $\omega=4500$ rpm (the maximum speed).

V. CONCLUSION

In this paper, an optimal design procedure of surface mounted PMSM is investigated. Firstly, an analytical model of PMSM is presented. This model is sufficiently accurate and fast to be used in the design optimization with stochastic methods like genetic algorithms. Then, the NSGA-II method is proposed to solve the highly nonlinear constrained multi-objective problem formed by two objectives (motor weight and total power loss) and four important constraints (demanded value of electromagnetic torque, maximum limit of back EMF, flux density saturation in stator/rotor yoke and saturation in stator tooth).

Finally, this design procedure, based on the proposed analytical model and NSGA-II algorithm, has been successfully applied for optimal design of 30 kW/1500 rpm PMSM. The obtained results show that the proposed methodology has a good accuracy and requires a reasonable computation time. Also, the Pareto fronts obtained from this procedure allows the designer to consider a good compromise between efficiency and weight of the motor in an effective manner. Moreover, this method can be used to design another types of machine, such as PMSM with external rotor.

REFERENCES

- [1] A. Cavagnino, M. Lazzari, F. Profumo, and A. Tenconi, "A comparison between the axial flux and the radial flux structures for PM motors," *IEEE Trans. Ind. Applicat.*, vol. 38, pp. 1517-1524, Nov. 2002.
- [2] S. Sonoda, Y. Takahashi, K. Kawagishi, N. Nishida, and S. Wakao, "Application of stepwise multiple regression to design optimization of electric machine," *IEEE Trans. Magn.*, vol. 43, pp. 1609-1612, Apr. 2007.
- [3] G. R. Slemon and X. Liu, "Modeling and design optimization of permanent magnet motors,"

Electric Machines & Power systems, vol. 20, pp. 71-92, 1992.

- [4] B. Nogarede, A. D. Kone, and M. Lajoie, "Modeling and simulation of inverter fed slotless permanent magnet machines," in *IMACS'91-13th World Congress on Computation and Applied Mathematics*, vol. 4, pp. 1529-1531, Jul. 1991.
- [5] Z. Q. Zhu, D. Howe, E. Bolte, and B. Ackermann, "Instantaneous magnetic field distribution in brushless permanent magnet dc motors, part I: open-circuit field," *IEEE Trans. Magn.*, vol. 29, pp. 124-135, Jan. 1993.
- [6] A. Chebak, P. Viarouge, and J. Cos, "Analytical model for design of high-speed slotless brushless machines with SMC stators," *IEEE Electric Machines & Drives Conference IEMDC '07*, vol. 1, pp. 159-164, May 2007.
- [7] S. Mendaci, M. R. Mekideche, and H. Allag, "Instantaneous analytical model of radial surface permanent magnet synchronous motor dedicated to optimal design," *IREMOS*, vol. 4, pp. 1542-1549, Aug. 2011.
- [8] Z. Q. Zhu and D. Howe, "Instantaneous magnetic field distribution in brushless permanent magnet dc motors, part III: effect of stator slotting," *IEEE Trans. Magn.*, vol. 29, pp. 143-151, Jan. 1993.
- [9] K. Deb, *Multi-Objective Optimization Using Evolutionary Algorithm*, Wiley, Chichester, 2001.
- [10] K. Deb, A. Pratap, S. Agarwal, and T. Meyarivan, "A fast and elitist multiobjective genetic algorithm: NSGA-II," *IEEE Trans. On Evolutionary Computation*, vol. 6, pp. 182-197, Apr. 2002.
- [11] M. T. Jensen, "Reducing the run-time complexity of multiobjective EAs: the NSGA-II and other algorithms," *IEEE Trans. On Evolutionary Computation*, vol. 7, pp. 503-515, Oct. 2003.
- [12] B. Sareni, J. Regnier, and X. Roboam, "A recombination and self-adaptation in multi-objective genetic algorithms," *Lectures Notes in Computer Science*, vol. 2936, pp. 115-127, 2004.



Sofiane Mendaci was born in Jijel, Algeria, in 1976. He received the B.S. degree from Jijel University, Algeria, in 2000, the M.S. degree from Paris XI University, France, in 2004, and the Ph.D. degree from Jijel University, Algeria, in 2013, all in Electrical Engineering. His research interests include design, modeling, and control of electrical machines.

He is currently an Assistant Professor in the Department of Electrical Engineering at the University of Guelma, Algeria.



Hicham Allag was born in Jijel, Algeria, in 1978. He received the B.S. degree from Jijel University, Algeria, in 2000, the M.S. degree from University of Constantine, Algeria, in 2004, and the Ph.D. degree from Grenoble University, France, in 2010, all in Electrical Engineering. His research interests include magnetic levitation and electromagnetic forces calculation.

He is an Associate Professor in the Department of Electrical Engineering at Jijel University, Algeria.



Mohamed Rachid Mekideche was born in Jijel, Algeria in 1957. He received the M.S. degree from the National Polytechnic School of Algiers, Algeria, in 1986, and the Ph.D. degree from Nantes University, France, in 1994, all in Electrical engineering. His research interests include analytical modeling and analysis of electrical machines.

He is now at the University of Jijel, as a Professor and Dean of the Engineering Faculty.